

## Interfacial strain effects in epitaxial multiferroic heterostructures of $\text{PbZr}_x\text{Ti}_{1-x}\text{O}_3/\text{La}_{0.7}\text{Sr}_{0.3}\text{MnO}_3$ grown by pulsed-laser deposition

Ionela Vrejoiu,<sup>1,a)</sup> Michael Ziese,<sup>2,a)</sup> Annette Setzer,<sup>2</sup> Pablo D. Esquinazi,<sup>2</sup> Balaji I. Birajdar,<sup>1</sup> Andriy Lotnyk,<sup>1</sup> Marin Alexe,<sup>1</sup> and Dietrich Hesse<sup>1</sup>

<sup>1</sup>Max Planck Institute of Microstructure Physics, Halle, D-06120, Germany

<sup>2</sup>Division of Superconductivity and Magnetism, University of Leipzig, D-04103 Leipzig, Germany

(Received 5 March 2008; accepted 20 March 2008; published online 17 April 2008)

Ferroelectric  $\text{PbZr}_x\text{Ti}_{1-x}\text{O}_3$  and ferromagnetic  $\text{La}_{0.7}\text{Sr}_{0.3}\text{MnO}_3$  films were grown on  $\text{SrTiO}_3(100)$  substrates in order to fabricate multiferroic epitaxial heterostructures. Multilayers of  $\text{PbZr}_{0.2}\text{Ti}_{0.8}\text{O}_3/\text{La}_{0.7}\text{Sr}_{0.3}\text{MnO}_3$  with 5 nm thin individual layers preserve good magnetic properties and have a transition temperature of  $\sim 320$  K. The variation of the magnetic coercive field of thin  $\text{La}_{0.7}\text{Sr}_{0.3}\text{MnO}_3$  films, sandwiched between  $\text{PbZr}_x\text{Ti}_{1-x}\text{O}_3$  films of increasing Zr content in the same epitaxial heterostructure, demonstrates the influence of the interfacial biaxial strain. © 2008 American Institute of Physics. [DOI: 10.1063/1.2908037]

$\text{PbZr}_x\text{Ti}_{1-x}\text{O}_3$  (PZT) thin films and PZT-based heterostructures (HSs) have stirred much interest owing to their excellent ferroelectric (FE) and piezoelectric properties.<sup>1</sup> An additional degree of versatility of PZT is that, by tuning the Zr/Ti ratio, the structure changes from tetragonal (for Ti-rich compositions) to rhombohedral and orthorhombic (for Zr-rich compositions). Consequently, the lattice parameters and the physical properties undergo important changes as well.<sup>2</sup> The hole-doped manganese oxides, such as  $\text{La}_{1-y}\text{Sr}_y\text{MnO}_3$  (LSMO), are another class of attractive perovskites due to the colossal magnetoresistance in the vicinity of the ferromagnetic (FM)-paramagnetic transition.<sup>3,4</sup> Hybrid structures combining FM and FE phases, including superlattices (SLs), have been investigated for their multiferroic functionalities and interfacial effects.<sup>4-7</sup> Here, we report on the influence of the interfacial strain exerted by thin PZT layers on adjacent LSMO layers in epitaxial LSMO/PZT multilayers, manifested in the modification of the coercive magnetic fields of the individual LSMO layers, resulting in stepped magnetization hysteresis curves.

The HSs were fabricated by pulsed-laser deposition (PLD), employing a KrF excimer laser ( $\lambda=248$  nm) following Ref. 8. Vicinal single crystalline  $\text{SrTiO}_3(100)$  (STO) substrates with a miscut angle of about  $0.1^\circ$  (CrysTec, Berlin) were used. Ceramic targets of  $\text{Pb}_{1.1}(\text{Zr}_x\text{Ti}_{1-x})\text{O}_3$  ( $x \cong 0.1, 0.2, 0.3, 0.52$ ) and  $\text{La}_{0.7}\text{Sr}_{0.3}\text{MnO}_3$  were employed and the PZT and LSMO layers were grown at a temperature of  $600^\circ\text{C}$  in 0.3 mbar oxygen and cooled down in 1 bar  $\text{O}_2$ .

Transmission electron microscopy (TEM) was performed on cross section samples (beam direction  $[010]$  STO), conventional TEM in a Philips CM20T at 200 keV primary energy, high resolution TEM (HRTEM) in a Jeol4010 at 400 kV, and Z-contrast imaging in a FEI TITAN 80–300 at 300 kV. Magnetic measurements were made with a superconducting quantum interference device magnetometer (Quantum Design, model MPMS7). Magnetic fields were applied along the  $[010]$  STO direction parallel to the HS plane. Macroscopic polarization hysteresis curves were acquired using a TF2000 Analyzer (AixaCCT).

Figure 1 shows an epitaxial multilayer with 15 bilayers of LSMO and PZT20/80 (i.e., PZT for  $x=0.2$ ), each layer  $\sim 5$  nm thin. The interfaces between the LSMO and PZT20/80 layers, although not entirely atomically flat, are coherent, as proven by Z-contrast scanning TEM (inset of Fig. 1).

FE measurements were performed on a 90 nm PZT20/80/70 nm LSMO bilayer, with Pt top electrodes ( $0.004$  mm<sup>2</sup>), giving a remnant polarization at 1 kHz of  $P_r = 80$   $\mu\text{C}/\text{cm}^2$ , which is slightly smaller than that measured on our coherently grown PZT20/80 films on top of  $\text{SrRuO}_3$ -coated STO(100).<sup>8</sup> Piezoforce microscopy (PFM) of a PZT20/80/LSMO multilayer grown on Nb-doped STO(100), similar to Fig. 1, indicated that the PZT layers exhibit stable polarization switching (not shown).

The magnetic hysteresis loops measured on a single LSMO film (5 nm) grown on STO(100) and on the PZT20/80/LSMO multilayer shown in Fig. 1 are displayed in Figs. 2(a) and 2(b), respectively. The magnetization at 5 K was about 0.55 T for all our single LSMO thin films with thick-

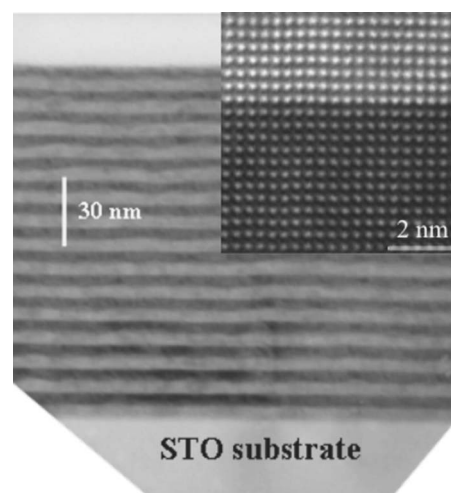


FIG. 1. TEM cross section micrograph of 15 PZT20/80/LSMO bilayers grown on STO(100), seen from  $[010]$  STO direction (bright layers are LSMO and dark contrast ones are PZT20/80). The inset is a Z-contrast scanning TEM image of one of the PZT20/80/LSMO interfaces in such a multilayer.

<sup>a)</sup> Authors to whom correspondence should be addressed. Electronic addresses: vrejoiu@mpi-halle.de and ziese@physik.uni-leipzig.de.

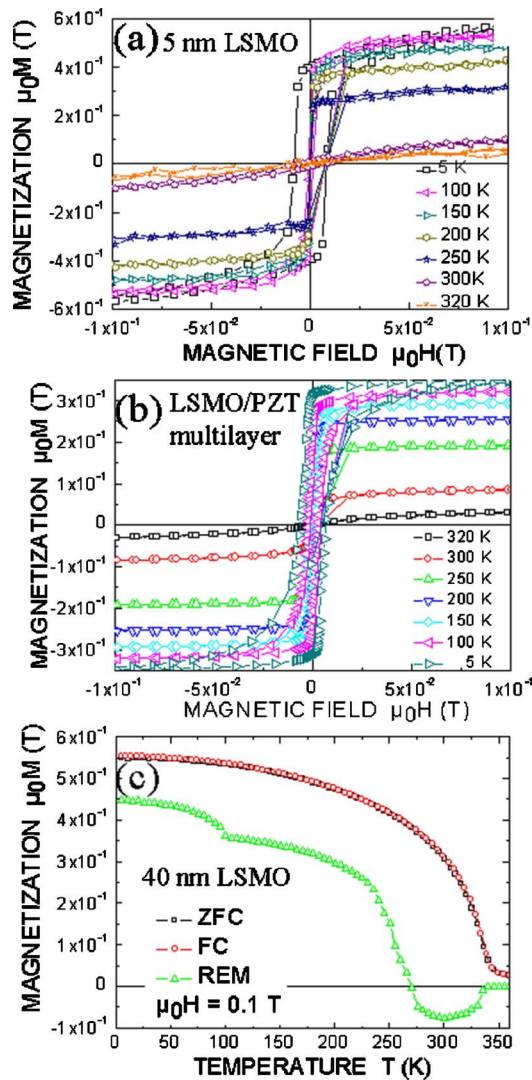


FIG. 2. (Color online) Hysteresis loops measured on (a) a  $\sim 5$  nm thin LSMO film at different temperatures and (b) a PZT/LSMO multilayer (shown in Fig. 1). (c) Magnetization dependence of temperature measured on the 40 nm thick LSMO film: ZFC, FC in 0.1 T, and at REM.

ness up to 40 nm and from the magnetization versus temperature curves we inferred a transition temperature  $T_C \leq 330$  K [see Fig. 2(c)]. This  $T_C$  is in good agreement with other reports on epitaxial ultrathin LSMO layers grown on STO(100) (Ref. 9) and slightly smaller than the value for bulk  $\text{La}_{0.7}\text{Sr}_{0.3}\text{MnO}_3$  crystals,  $T_C \cong 370$  K.<sup>3</sup> Reports on LSMO/BaTiO<sub>3</sub> SLs showed that their  $T_C$  was significantly

lower ( $\leq 290$  K) than that of single LSMO films.<sup>10</sup> The same reduction of  $T_C$  was also observed for  $\text{La}_{0.7}\text{Ca}_{0.3}\text{MnO}_3$  (LCMO)/STO multilayers with respect to LCMO single epitaxial layers grown on STO(100).<sup>11</sup> Our PZT 20/80/LSMO multilayers had  $T_C \cong 320$  K and were different from our single LSMO films in that they had 40% reduction of the remnant magnetization (0.3 T at 5 K) (see Figs. 2(a) and 2(b)). A similar magnetization reduction was observed for the LSMO/BaTiO<sub>3</sub> SLs (Ref. 10) and LCMO/STO multilayers.<sup>11</sup> It has often been attributed to magnetic disorder at the interfaces, either generated by epitaxial strain or by phase separation.<sup>12–15</sup> We observed no phase separation or compositional inhomogeneity at the PZT20/80/LSMO interfaces.

We consider as prevailing the effect of in-plane tensile strain experienced by the ultrathin LSMO layers sandwiched between PZT20/80 layers. For FM and FE perovskite films the epitaxial interfacial strain can affect the phase transition temperatures, saturation magnetization and polarization, coercive fields, transport properties, and degree of anisotropy.<sup>12,15–19</sup> To affect the  $T_C$  of FM LSMO layers by epitaxial strain we grew multilayers in which the LSMO films were sandwiched between tetragonal *c*-axis oriented FE PZT layers with increasing Zr content. Such HSs are given in Fig. 3, which shows six-layer HSs of PZT30/70/LSMO/PZT20/80/LSMO/PZT10/90/LSMO [Fig. 3(a)] and PZT52/48/LSMO/PZT30/70/LSMO/PZT10/90/LSMO [Fig. 3(b)], grown on STO(100). For the HS from Fig. 3(a) the thickness of each LSMO layer is  $\sim 10$  nm and of each PZT layer is  $\sim 30$  nm, and for the HS in Fig. 3(b), each LSMO layer is  $\sim 20$  nm and each PZT layer is  $\sim 100$  nm. HRTEM (not shown) of the HS from Fig. 3(a) confirmed the high quality of the LSMO/PZT interfaces and the absence of intermixing or nanoprecipitates, as found elsewhere.<sup>20,21</sup> The PZT layers are all tetragonal and *c*-axis oriented. With increasing Zr/Ti ratio, they have larger in-plane lattice parameters ( $a_{\text{PZT10/90}} = 3.93$  Å,  $a_{\text{PZT20/80}} = 3.954$  Å,  $a_{\text{PZT30/70}} = 3.98$  Å,  $a_{\text{PZT52/48}} = 4.05$  Å, *bulk* room temperature values), all larger than  $a_{\text{LSMO}} = 3.875$  Å (pseudocubic)<sup>21</sup> and  $a_{\text{STO}} = 3.905$  Å. Thus, the PZT layers exert a gradually increasing in-plane stress on the adjacent LSMO layers. Hence, the magnetization and  $T_C$  of the three LSMO layers undergo significant alterations. The hysteresis loops measured on HSs shown in Figs. 3(a) and 3(b) are given in Figs. 4(a) and 4(b), respectively. The magnetization hysteresis in Fig. 4(a) clearly shows at least two steps, indicating that there are at least two values of the magnetic field at which independent magnetization switching

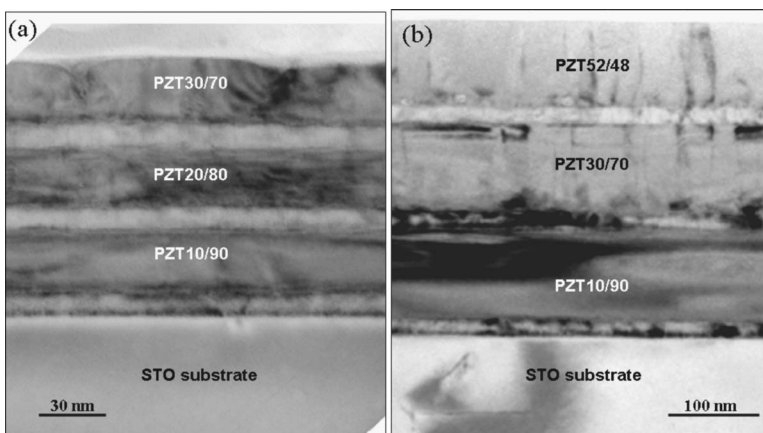


FIG. 3. TEM cross section micrographs of the six-layer PZT/LSMO HSs grown on STO(100), with PZT layers of different Zr/Ti ratios (as indicated on the micrographs). The first, third, and fifth layers starting from STO are LSMO.

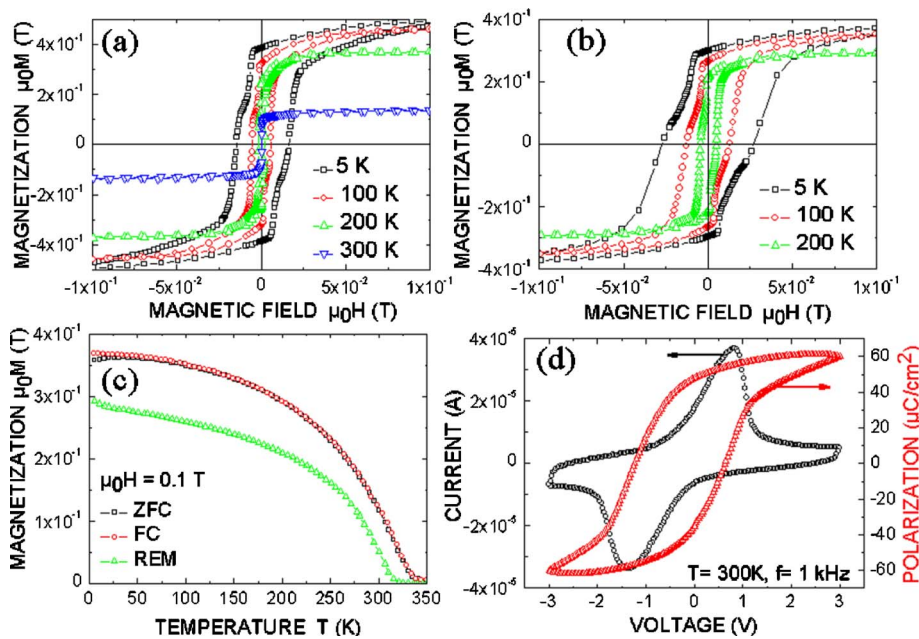


FIG. 4. (Color online) Magnetic measurements of the six-layer PZT/LSMO HSs: magnetization hysteresis at various temperatures for (a) the HS from Figs. 3(a) and (b) for the HS from Fig. 3(b). (c) Magnetization dependence of temperature and (d) switching current and polarization hysteresis curves, both of the HS from Fig. 3(b).

occurs.<sup>16,19,20</sup> This is likely due to the fact that the three LSMO layers of the six-layer HS experience different values of in-plane stress, which affects their structure and thus results in slightly different coercive field values.<sup>19</sup> Such steps are more clearly discerned for the magnetization hysteresis curves in Fig. 4(b), indicating that the  $H_C$  are larger and better separated, and the remnant and saturation magnetization are slightly smaller for the HS shown in Fig. 3(b). This is in accord with the fact that the LSMO layers of this HS should be subjected to larger tensile interfacial strain than the LSMO layers of the structure shown in Fig. 3(a). We assume that in both HSs the LSMO layer between the STO and the PZT10/90 layer has the lowest coercive field and switches first, as it is least distorted. For the HS from Fig. 3(b), the magnetization versus temperature curves for zero-field cooling (ZFC), for FC, and for the remnant magnetization [warming up in zero field after cooling in 0.1 T, remanence (REM)] are shown in Fig. 4(c). The effective remnant magnetic moment vanishes at about 320 K. We measured FE polarization hysteresis loops for the sample shown in Fig. 3(b), at 1 kHz and room temperature [Fig. 4(d)]. However, the measured polarization hysteresis loop of this HS solely arises from the switching of the topmost PZT52/48 layer, the other two PZT layers of the HS being sandwiched between short-circuited LSMO layers.<sup>6,22</sup> Hence, magnetoelectric measurements of the as-grown HSs are not possible. Selective etching of LSMO and sample patterning are required, work that is underway.

In summary, epitaxial HSs of FE PZT and FM  $\text{La}_{0.7}\text{Sr}_{0.3}\text{MnO}_3$  layers were grown and characterized. The individual layers retain their respective FE and FM properties. Nevertheless, the FE and FM layers influence each other, primarily by the interfacial strain they experience due to their lattice mismatches during growth. More subtle effects may arise from the possible interfacial magnetoelectric coupling of the FM and FE layers, which requires further investigation.

We thank Dr. E. Pippel for Z-contrast STEM, Dr. B. J. Rodriguez for PFM, and Ms. S. Swatek for preparation of

TEM samples. Work was supported by DFG via SFB762.

<sup>1</sup>J. F. Scott and C. A. P. D. Araujo, *Science* **246**, 1400 (1989).

<sup>2</sup>E. Sawaguchi, *J. Phys. Soc. Jpn.* **8**, 615 (1953).

<sup>3</sup>A. Urushibara, Y. Moritomo, T. Arima, A. Asamitsu, G. Kido, and Y. Tokura, *Phys. Rev. B* **51**, 14103 (1995).

<sup>4</sup>K. Dörr, *J. Phys. D* **39**, 125 (2006).

<sup>5</sup>W. Eerenstein, N. D. Mathur, and J. F. Scott, *Nature (London)* **442**, 759 (2006).

<sup>6</sup>A. R. Chaudhuri, R. Ranjith, S. B. Krupanidhi, R. V. K. Mangalam, A. Sundaresan, S. Majumdar, and S. K. Ray, *J. Appl. Phys.* **101**, 114104 (2007).

<sup>7</sup>P. Murugavel, M. P. Singh, W. Prellier, B. Mercey, Ch. Simon, and B. Raveau, *J. Appl. Phys.* **97**, 103914 (2005).

<sup>8</sup>I. Vrejoiu, G. Le Rhun, L. Pintilie, D. Hesse, M. Alexe, and U. Gösele, *Adv. Mater. (Weinheim, Ger.)* **18**, 1657 (2006).

<sup>9</sup>F. Tsui, M. C. Smoak, T. K. Nath, and C. B. Eom, *Appl. Phys. Lett.* **76**, 2421 (2000).

<sup>10</sup>P. Murugavel and W. Prellier, *J. Appl. Phys.* **100**, 023520 (2006).

<sup>11</sup>M.-H. Jo, N. D. Mathur, J. E. Evetts, M. G. Blamire, M. Bibes, and J. Fontcuberta, *Appl. Phys. Lett.* **75**, 3689 (1999).

<sup>12</sup>M. G. Blamire, B.-S. Teo, J. H. Durrell, N. D. Mathur, Z. H. Barber, J. L. McManus Driscoll, L. E. Cohen, and J. E. Evetts, *J. Magn. Magn. Mater.* **91**, 359 (1999).

<sup>13</sup>M. Ziese, H. C. Semmelhack, and K. H. Han, *Phys. Rev. B* **68**, 134444 (2003).

<sup>14</sup>M. Bibes, Ll. Balcells, S. Valencia, J. Fontcuberta, M. Wojcik, E. Jedryka, and S. Nadolski, *Phys. Rev. Lett.* **87**, 067210 (2001).

<sup>15</sup>L. Abad, V. Laukhin, S. Valencia, A. Gaup, W. Gudat, Ll. Balcells, and B. Martínez, *Adv. Funct. Mater.* **17**, 3918 (2007).

<sup>16</sup>Y. Suzuki, H. Y. Hwang, S.-W. Cheong, and R. B. van Dover, *Appl. Phys. Lett.* **71**, 140 (1997).

<sup>17</sup>B. Wiedenhorst, C. Höfener, Y. Lu, J. Klein, L. Alff, R. Gross, B. H. Freitag, and W. Mader, *Appl. Phys. Lett.* **74**, 3636 (1999).

<sup>18</sup>K. J. Choi, M. Biegalski, Y. L. Li, A. Sharan, J. Schubert, R. Uecker, P. Reiche, Y. B. Chen, X. Q. Pan, V. Gopalan, L.-Q. Chen, D. G. Schlom, and C. B. Eom, *Science* **306**, 1005 (2004).

<sup>19</sup>M. Przybylski, J. Grabowski, F. Zavaliche, W. Wulfhekkel, R. Scholz, and J. Kirschner, *J. Phys. D* **35**, 1821 (2002).

<sup>20</sup>J.-H. Liao and T.-B. Wu, *Electrochem. Solid-State Lett.* **10**, P27 (2007).

<sup>21</sup>O. I. Lebedev, J. Veerbeeck, G. Van Tendeleo, C. Dubordieu, and P. Chaudouet, *J. Appl. Phys.* **94**, 7646 (2003).

<sup>22</sup>In our PZT20/80/LSMO multilayers (from Fig. 1) and HSs (from Fig. 3), LSMO layers are in contact on the sides of the substrate due to the PLD fabrication and thus are "short circuited."